

T. Brey · J. Gutt · A. Mackensen · A. Starmans

## Growth and productivity of the high Antarctic Bryozoan *Melicerita obliqua*

Received: 27 February 1998 / Accepted: 8 May 1998

**Abstract** We analysed growth of the Antarctic bryozoan *Melicerita obliqua* (Thornely, 1924) by x-ray photography and stable isotope analysis. *M. obliqua* colonies form one segment per year, thus attaining maximum length of about 200 mm within 50 years. In the Weddell and Lazarev Seas, annual production/biomass ratio of *M. obliqua* is 0.1 yr<sup>-1</sup>, which is in the range of other Antarctic benthic invertebrate populations. Production amounts to 3.34 mg C<sub>org</sub> m<sup>-2</sup> yr<sup>-1</sup> and 90.6 mg ash m<sup>-2</sup> yr<sup>-1</sup> on the shelf (100 to 600 m water depth), and to 0.13 mg C<sub>org</sub> m<sup>-2</sup> yr<sup>-1</sup> and 36.8 mg ash m<sup>-2</sup> yr<sup>-1</sup> on the slope (600 to 1250 m water depth).

### Introduction

The cheilostome bryozoan *Melicerita obliqua* (Thornely, 1924; family Cellariidae) is one of the most conspicuous organisms of the high-Antarctic shelf and slope benthos. Its blade-shaped colonies (with zooids on both blades) are encountered frequently in trawl samples, and underwater video and still photographs often show dense patches of *Melicerita* colonies (Winston 1983; Gutt and Starmans 1998).

*Melicerita obliqua* exhibits macroscopically visible nodes which separate adjacent colony segments (Fig. 1), but it is unclear if these nodes are formed at regular intervals in time (Ryland 1976). The colonies of many calcified bryozoan species exhibit similar visible nodes or bands (e.g. Winston 1983; Cook 1985). So far, however, the annual formation of growth bands has been verified only for two boreal species, *Flustra foliacea* (South Wales, Stebbing 1971) and *Pentapora foliacea* (Irish Sea,

Pätzold et al. 1987), and for one Antarctic species, *Cellarinella watseri* (Signy Island, Barnes 1995) which is closely related to *M. obliqua*.

Our study of *Melicerita obliqua* focuses on three aims: (i) evaluation of colony age; (ii) development of a growth pattern model; and (iii) the estimation of biomass and production on the shelf and slope of both the Weddell and Lazarev Seas.

### Methods

#### Sampling

Data on abundance and size distribution of *Melicerita obliqua* on the shelf and slope of both the Weddell and Lazarev Seas were obtained from underwater still photographs. During "Polarstern" expeditions ANT III (1985), ANT VI (1988), ANT VII (1989) and ANT IX (1991) 3877 photographs, each covering either 0.9 or 0.6 m<sup>2</sup> of sea bottom (3304 m<sup>2</sup> in total), were taken at 55 stations between 100 and 1250 m water depth (Gutt and Starmans 1998). Colonies of *M. obliqua* visible on these photos were counted to compute average abundance. We used photographs taken at three shelf stations with frequent occurrence of *M. obliqua* (Table 1) to establish a size-frequency distribution. The colonies of *M. obliqua* do not grow vertically, but at an acute angle to the sea bottom, so that larger specimens are situated almost parallel to the sediment surface. The photographs were projected on a 90 × 90 cm square, and the length of all colonies fully visible was measured to the lower 5 mm. Specimens for growth analysis were collected from benthic samples taken by various types of gear during five expeditions (Table 1). None of the colonies sampled was complete, i.e. our sample consisted of 83 colony fragments of various size.

#### Morphometrics

We determined segment length  $L_x$  of segment  $x$  from the average of the lengths at both the convex ( $L_{co}$ ) and concave ( $L_{cv}$ ) sides of the colony (see Fig. 1):

$$L_x = (L_{co} + L_{cv})/2 ,$$

and the corresponding segment area  $A_x$  by multiplying segment width  $W_x$  at the base of the segment with segment length  $L_x$ :

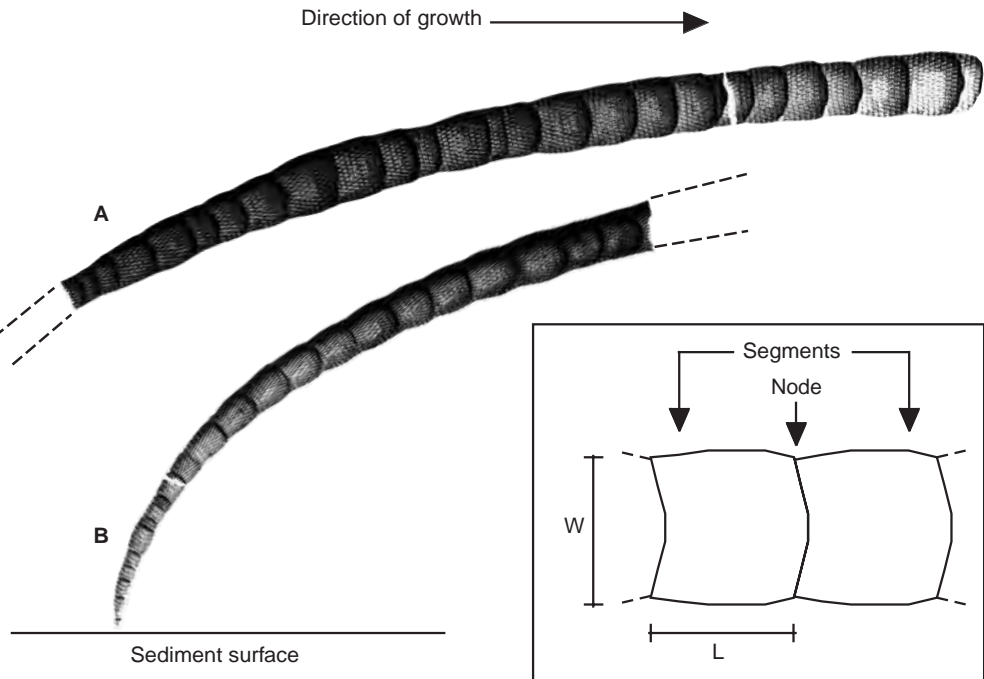
$$A_x = W_x \cdot L_x .$$

Relations between colony area (i.e. the sum of segment areas of a colony) and colony mass were based on 26 fragments sampled in

Communicated by O. Kinne, Oldendorf/Luhe

T. Brey (✉) · J. Gutt · A. Mackensen · A. Starmans  
Alfred Wegener Institute for Polar and Marine Research,  
P.O. Box 120161, D-27576 Bremerhaven,  
Germany

**Fig. 1** *Melicerita obliqua*. X-ray photographs of two colonies sampled in March 1996. **A** Colony fragment (25 segments, 131 mm length) has lost the oldest segments, but shows the recent growth zone. **B** Fragment (23 segments, 95 mm length) has lost the most recent segments, but shows the oldest segments. Both fragments are arranged in approximate natural living position. Inset: schematic drawing of two adjacent segments indicating segment length (*L*) and width (*W*) measurements



1996. Dry mass was determined after drying for 24 h at 60 °C, ash content after 24 h at 500 °C.

#### Node formation

Two large colony fragments were x-ray photographed to check whether the nodes visible at the colony surface resemble distinct internal structures of the colony.

The ratio of the stable oxygen isotopes  $^{18}\text{O}$  and  $^{16}\text{O}$  ( $\delta^{18}\text{O}$ ) in shell carbonate depends on seawater isotope composition and temperature during shell deposition. Deep-sea isotope composition is rather stable on a biological time scale, hence  $\delta^{18}\text{O}$  in calcitic shell can be related to ambient temperature via the paleotemperature equations of Epstein et al. (1953) and McCrea (1950). The ratio of the stable carbon isotopes  $^{13}\text{C}$  and  $^{12}\text{C}$  in shell carbonate depends mainly on  $\delta^{13}\text{C}$  of seawater bicarbonate mediated by primary production (Emrich et al. 1970; Krantz et al. 1987). Therefore  $\delta^{18}\text{O}$  and  $\delta^{13}\text{C}$  can be used to analyse seasonality of growth in living or fossil calcareous species (see Krantz et al. 1987; Wefer and Berger 1991). For isotope analysis, carbonate samples of 50 to 100 µg each were drilled from the colony using a small dental drill (bit size 0.5 mm). We applied two sampling strategies: (i) a statistical approach where samples collected from nodes were compared with samples collected from segments of several colonies by two-way analysis of variance (ANOVA; independent variables were location of sample and colony specimen); and (ii) a high

resolution array of narrowly spaced subsequent drill holes across several adjacent segments of one colony to identify the seasonal cycle in isotope ratios.

We measured stable oxygen and carbon isotopes of the carbonate samples with a Finnigan MAT251 mass spectrometer coupled to an automatic carbonate preparation device. The precision of measurements is better than  $\pm 0.06\text{\textperthousand}$  for  $\delta^{13}\text{C}$  and  $\pm 0.08\text{\textperthousand}$  for  $\delta^{18}\text{O}$ , based on routine measurements of a laboratory working standard. Data are related to the Pee Dee belemnite (PDB) standard through repeated analyses of isotopic reference material (NBS 19) from the National Bureau of Standards (Hut 1987).

#### Colony growth

Based on the 83 colony fragments available, we applied a two-step approach to model growth functions. In a first step, a regression (geometric mean regression model according to Ricker 1975) between length  $L_x$  (or area  $A_x$ ) of segment  $x$  and the length  $L_{x+1}$  (area  $A_{x+1}$ ) of the subsequent segment  $x + 1$  was established:

$$L_{x+1} = a + b \cdot L_x$$

$$A_{x+1} = a + b \cdot A_x .$$

Then, using the smallest length (area) measured as an offset value ( $L_1, A_1$ ), average segment length (area) of subsequent segments was

for size-frequency measurements. Stations where photos were taken for abundance counts only are not included in this table

**Table 1** Stations sampled in the Weddell and Lazarev Seas by Agassiz trawl (AGT), epibenthic sledge (EBS) and multi-box corer (MG) for growth analysis and by underwater photography (UWF)

Year	Expedition	Station No.	Lat. (S)	Long. (W)	Depth (m)	Sampling method
1983	ANT I/2	129	70°29.9'	8°7.3'	286	AGT
1983	ANT I/2	210	72°55.1'	19°41.8'	445	AGT
1996	ANT XIII/3	006	71°31.7'	13°38.2'	279	AGT
1996	ANT XIII/3	007	71°26.5'	13°42.2'	223	EBS
1996	ANT XIII/3	025	71°23.1'	14°19.7'	628	AGT/MG
1988	ANT VI/3	396	71°17.0'	13°46.8'	529	UWF
1989	ANT VII/4	245	74°39.9'	29°39.9'	508	UWF
1991	ANT IX/3	220	70°24.0'	6°2.0'	130	UWF

computed iteratively using the above regression functions. The cumulative values of  $L_{1 \rightarrow x}$  ( $A_{1 \rightarrow x}$ ) represent average colony length (area) after growing  $x$  segments. Growth in  $C_{org}$  and inorganic compounds was computed by converting segment area to mass using the appropriate morphometric regression equations.

### Productivity

We computed somatic productivity and production using the mass-specific growth rate method according to Crisp (1984). The annual somatic production-to-biomass ratio  $P/B$  was computed from (i) the size-frequency distribution, (ii) the size-growth function and (iii) the size-mass relation by

$$P/B = \sum N_i \cdot M_i \cdot G_i / \sum N_i \cdot M_i \text{ [yr}^{-1}\text{]},$$

where  $N_i$  is the number of individuals in size class  $i$ ,  $M_i$  is the mean individual body mass in size class  $i$ , and  $G_i$  is the corresponding annual mass-specific growth rate (see Brey et al. 1990; Brey 1991 for detailed explanations).

Annual production per square meter was computed by multiplying the above  $P/B$  ratio with an estimate of average biomass  $B$ . This estimate was derived from mean abundance computed from the underwater still photographs,  $N_{foto}$ , and from mean body mass  $M_{mean}$  in the size-frequency sample:

$$P = P/B \cdot M_{mean} \cdot N_{foto} \text{ [mg m}^{-2}\text{y}^{-1}\text{].}$$

## Results

### Growth band formation

The nodes separating the segments of the colonies are clearly visible in the x-ray photograph as dark bands indicating material of higher density (Fig. 1).

Log-transformed stable isotope data of 30 nodes and 58 segments from three colonies were compared statistically. The  $\delta^{18}\text{O}$  values of nodes and segments did not differ significantly ( $P = 0.954$ ), whereas  $\delta^{13}\text{C}$  was significantly higher ( $P < 0.001$ ) in nodes (mean = 1.496) than in segments (mean = 1.249). The colony specimen affected neither  $\delta^{18}\text{O}$  nor  $\delta^{13}\text{C}$ . A stable-isotope, high-resolution array across five adjacent segments of one colony fragment revealed a distinct cycle in  $\delta^{13}\text{C}$  (low in segments, high in nodes), but not in  $\delta^{18}\text{O}$  (Fig. 2). The  $\delta^{13}\text{C}$  data indicate that nodes are produced annually.

### Abundance, size-frequency distribution and morphometric relations

Abundance of *Melicerita obliqua* was highly variable among stations, but significantly lower on the slope (600 to 1250 m water depth; mean 0.3 colonies  $\text{m}^{-2}$ ; range 0 to 2.8 colonies  $\text{m}^{-2}$ , 998 photos, 15 stations) than on the shelf (100 to 600 m water depth; mean 7.7 colonies  $\text{m}^{-2}$ ; range 0 to 262 colonies  $\text{m}^{-2}$ , 2879 photos, 40 stations) (ANOVA,  $\alpha = 0.05$ ). The size distributions from the three stations did not differ significantly (Kolmogorov-Smirnov test,  $\alpha = 0.05$ ). The pooled distribution (1095 individuals measured, Fig. 3) indicates that the major part of the population is < 100 mm in length, although a few individuals can grow beyond 200 mm length.

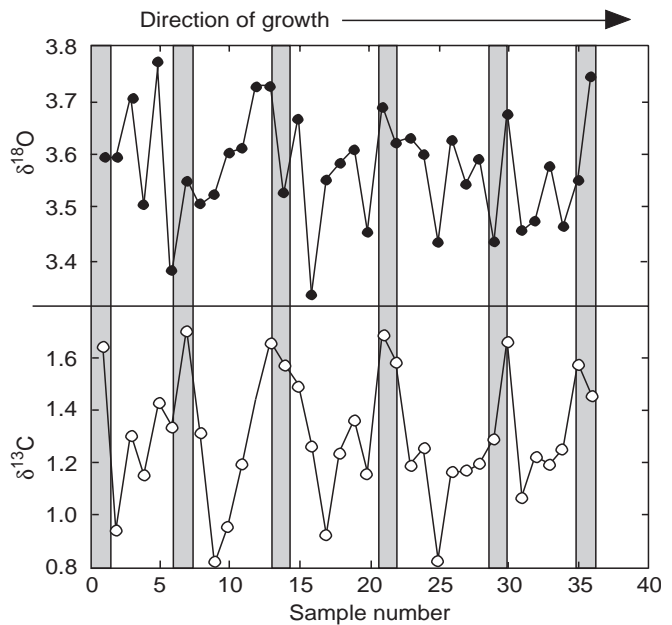


**Fig. 2** *Melicerita obliqua*. High spatial resolution isotope samples (36 samples across five adjacent segments). Shaded bars represent nodes

Segment length was much more variable than segment area (see Fig. 4), therefore the latter was used to establish mass-size relations. Ash free dry mass was on average 8.04% of dry mass;  $C_{org}$  was assumed to be 50% of ash free dry mass (see e.g. Salonen et al. 1976). The relations between  $C_{org}$ , ash and colony area ( $A$ ) were linear:

$$\begin{aligned} C_{org} &= -0.011 + 0.052 \cdot A; N = 31; \\ r^2 &= 0.986 \text{ [mg, mm}^2\text{]} \end{aligned} \quad (1)$$

$$\begin{aligned} \text{ash} &= -0.873 + 1.200 \cdot A; N = 31; \\ r^2 &= 0.988 \text{ [mg, mm}^2\text{]}. \end{aligned} \quad (2)$$

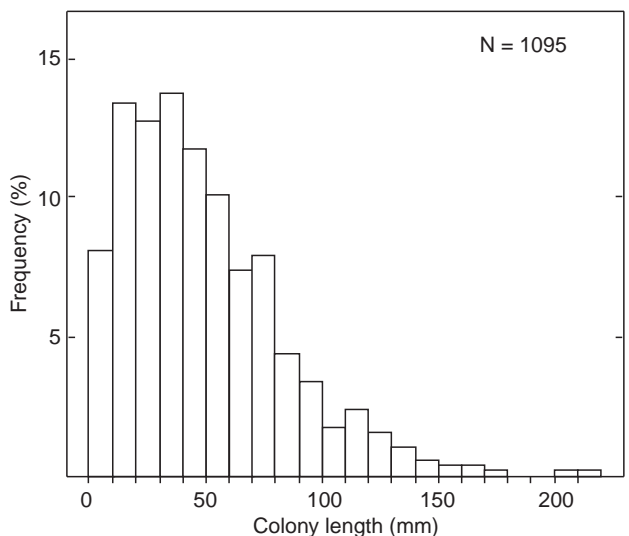


**Fig. 3** *Melicerita obliqua*. Size-frequency distribution from photographs taken at three stations (see Table 1)

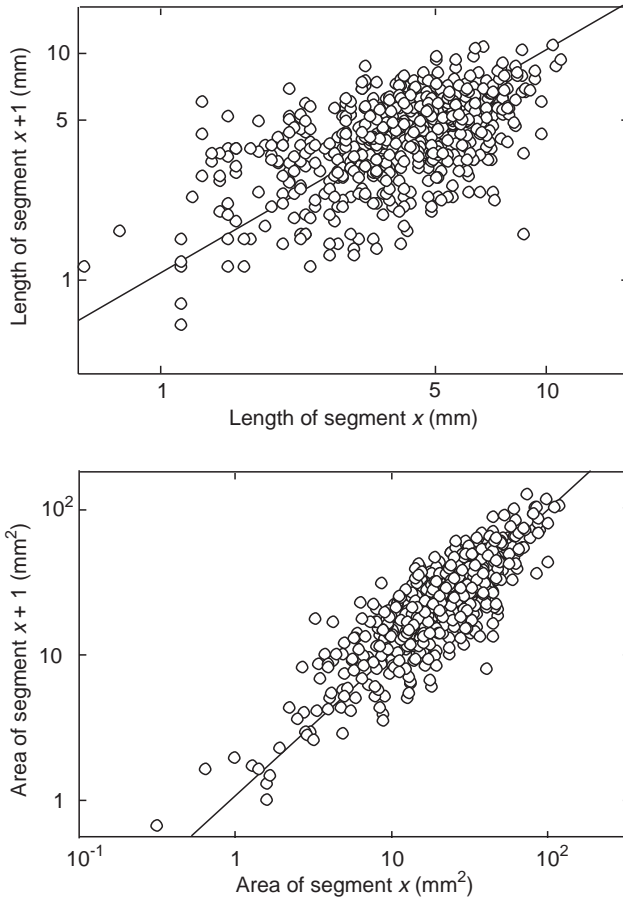


**Fig. 4** *Melicerita obliqua*. Relation between length  $L_x$  (area  $A_x$ ) of segment  $x$  and length  $L_{x+1}$  (area  $A_{x+1}$ ) of subsequent segment  $x + 1$ . Geometric mean models according to Ricker (1975); see Eqs. 3 and 4

#### Colony growth

The number of segments per colony fragment ranged between 3 and 25. From 594 pairs of segment length (area) measurements  $L_x$  and  $L_{x+1}$  ( $A_x$  and  $A_{x+1}$ ) we derived the log-log functions (Fig. 4):

$$\log(L_{x+1}) = 0.013 + 0.986 \cdot \log(L_x); \\ N = 594; r^2 = 0.312 \quad (3)$$

$$\log(A_{x+1}) = 0.084 + 0.953 \cdot \log(A_x); \\ N = 594; r^2 = 0.712, \quad (4)$$

which gave a better fit than the regression based on raw data.

We used the coefficients of these functions together with the offset values  $L_1 = 2.79$  mm and  $A_1 = 0.48$  mm<sup>2</sup> to iteratively compute colony growth curves up to 50 segments ( $S$ ) shown in Fig. 5. These curves are described best by second and third order polynomials:

$$L = -0.118 + 2.790 \cdot S + 0.021 \cdot S^2; \\ N = 50; r^2 = 0.999 \quad (5)$$

$$A = 8.8897 - 2.277 \cdot S + 0.2288 \cdot S^2 - 0.002 \cdot S^3; \\ N = 50; r^2 = 0.999. \quad (6)$$

Introducing Eqs. 1 and 2 into Eq. 6 resulted in growth curves for  $C_{\text{org}}$  and ash:

$$C_{\text{org}} = 0.465 - 0.312 \cdot S + 0.015 \cdot S^2 + 0.00012 \cdot S^3; N = 50; r^2 = 0.999 \quad (7)$$

$$\text{Ash} = 10.670 - 1.858 \cdot S + 0.346 \cdot S^2 + 0.00283 \cdot S^3; N = 50; r^2 = 0.999. \quad (8)$$

Surface  $A$  can be converted into number of zooids by the average factor of 2.11 zooids mm<sup>-2</sup> (SD = 0.29;  $N = 15$  samples). This factor has to be doubled when total number of zooids per segment is computed, because zooids cover both sides of the colony blade.

#### Productivity

Assuming a growth rate of one segment per year (see “Discussion”), we computed age corresponding to the midlength of each size class of the frequency distribution (Fig. 3) by the inverse of Eq. 5:

$$S = 0.488 + 0.325 \cdot L - 0.0004 \cdot L^2; r^2 = 0.999, \quad (9)$$

and colony mass per size class by the regressions:

$$\log(C_{\text{org}}) = -2.847 + 1.969 \cdot \log(L); \\ r^2 = 0.998 [\text{mg, mm}] \quad (10)$$

$$\log(\text{Ash}) = -0.759 + 1.635 \cdot \log(L); \\ r^2 = 0.984 [\text{mg, mm}], \quad (11)$$

which were derived from Eqs. 5, 7 and 8. Mass-specific growth rates were computed from the first derivative of Eqs. 7 and 8.

Annual  $P/B$  ratio amounted to 0.101 and 0.096 for  $C_{\text{org}}$  and ash, respectively. From the frequency distribution average body mass  $M_{\text{mean}}$  was estimated to be 4.29 mg  $C_{\text{org}}$  and 122.51 mg ash. Average abundance of *Melicerita obliqua* was 7.7 m<sup>-2</sup> on the shelf (100 to 600 m) and 0.3 m<sup>-2</sup> on the slope (600 to 1250 m). Hence average biomass amounts to:

$$\text{shelf: } B_{\text{org}} = 4.29 \cdot 7.7 = 33.03 \text{ mg } C_{\text{org}} \text{ m}^{-2}$$

$$B_{\text{ash}} = 122.51 \cdot 7.7 = 943.33 \text{ mg ash m}^{-2}$$

$$\text{slope: } B_{\text{org}} = 4.29 \cdot 0.3 = 1.29 \text{ mg } C_{\text{org}} \text{ m}^{-2}$$

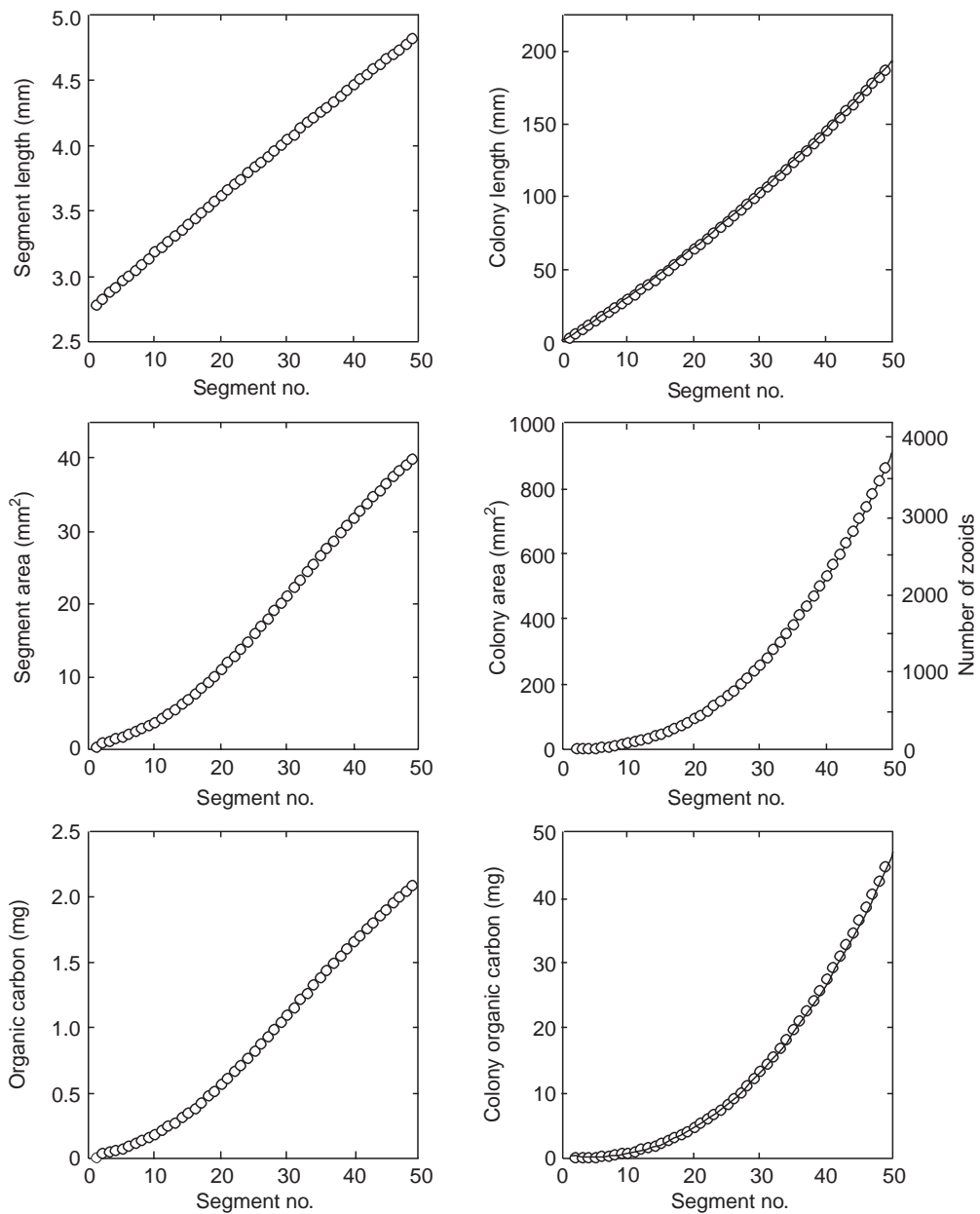
$$B_{\text{ash}} = 122.51 \cdot 0.3 = 36.75 \text{ mg ash m}^{-2}, \quad (12)$$

and annual production is estimated to be:

$$\text{shelf: } P_{\text{org}} = 0.101 \cdot 33.03 = 3.34 \text{ mg } C_{\text{org}} \text{ m}^{-2} \text{ yr}^{-1} \\ P_{\text{ash}} = 0.096 \cdot 943.33 = 90.56 \text{ mg ash m}^{-2} \text{ yr}^{-1}$$

$$\text{slope: } P_{\text{org}} = 0.101 \cdot 1.29 = 0.13 \text{ mg } C_{\text{org}} \text{ m}^{-2} \text{ yr}^{-1} \\ P_{\text{ash}} = 0.096 \cdot 36.75 = 3.53 \text{ mg ash m}^{-2} \text{ yr}^{-1}. \quad (13)$$

**Fig. 5** Average segment length (area, mass) and colony length (area, mass, number of zooids) in relation to segment number ( $S$ ), i.e. age in years. Data derived from Eqs. 3 and 4. Second and third degree polynomials are fitted to the colony data (all coefficients  $P < 0.001$ ); see Eqs. 5, 6 and 7



## Discussion

### Growth and age

The stable isotope data (Fig. 2) exhibit a distinct oscillation in  $\delta^{13}\text{C}$  which coincides with the segment pattern of *Melicerita obliqua*, indicating segment formation during periods of low  $\delta^{13}\text{C}$ , i.e. periods of high primary production (austral summer), and node formation during periods of high  $\delta^{13}\text{C}$  (winter). We failed to detect a similar profile in  $\delta^{18}\text{O}$ , presumably due to the small annual range ( $-1.8$  to  $-1.0^\circ\text{C}$ ) and strong short-term variability of water temperature on the Weddell Sea shelf (see Arntz et al. 1992). Seasonal growth in an environment with no distinct annual cycle

in temperature (Arntz et al. 1992) but extremely seasonal food input (von Bodungen et al. 1988; Bathmann et al. 1991) supports the hypothesis that seasonal growth patterns in Antarctic suspension feeders are more closely coupled to food availability than to water temperature (Clarke and North 1991; Brey and Clarke 1993; Barnes 1995).

The growth functions computed here (Fig. 5) describe average growth of *Melicerita obliqua*. Growth in colony length is almost linear ( $4.5 \text{ mm yr}^{-1}$  on average), whereas growth in colony area and mass is distinctly exponential. Our segment measurements, however, indicate high interannual variability in growth, independent of colony age (Fig. 4), as also found in *Cellarinella watersi* (Barnes 1995). This pattern is most likely related to interannual variability in primary production

(e.g. El-Sayed 1988; Smetacek et al. 1990) and hence food availability.

The size–frequency distribution of *Melicerita obliqua* (Fig. 3) indicates that colonies frequently reach ages between 20 and 30 years (60 to 100 mm length), whereas a few individuals may grow for over 50 years (> 200 mm length; > 3800 zooids). Iterative backcalculation of segment length with Eq. 3 indicates that the colony fragment shown in Fig. 1A lost 10 to 14 segments, i.e. the complete colony consisted of 35 to 39 segments (= 35 to 39 years of age).

*Melicerita obliqua* grows distinctly slower ( $4.5 \text{ mm yr}^{-1}$ ) than the boreal species *Flustra foliacea* ( $15 \text{ mm yr}^{-1}$ , max. age  $\approx 12$  yr, Stebbing 1971) and *Pentapora foliacea* ( $20 \text{ mm yr}^{-1}$ , max. age  $\geq 3$  yr, Pätzold et al. 1987). Barnes (1995) computed the growth rate of the Antarctic species *Cellarinella watseri* (max. age  $\approx 9$  yr) and *Alloeflustra tenuis* (max. age  $\approx 26$  yr) at Signy Island (40 m depth) by plotting annual increase in dry mass ( $\delta DM$ ) versus initial dry mass (DM). From his Fig. 3 we can infer that the slope of the  $\log(\delta DM)$ – $\log(DM)$  relation is about 0.9 in both species. In *M. obliqua*, the slope of the same relation computed from Eq. 7 or Eq. 8 (growth in  $C_{\text{org}}$  or ash) is only 0.6, indicating a distinctly lower rate of growth which may be explained by the lower food input to the Antarctic shelf benthos compared to shallow water sites around the South Orkney Islands (see El-Sayed 1988; Schalk et al. 1993).

### Productivity and production

The major weakness of our production calculation is the reliability of the size–frequency distribution obtained from underwater photographs (Fig. 3). As stated above, the colony blades of *Melicerita obliqua* are curved towards the sea bottom and grow at an acute angle to the sediment surface. Therefore, the vertical perspective of the camera makes the colony blade appear shorter, thus leading to underestimation of true colony length. The smaller the colony is the stronger the bias. Moreover, smaller colonies are more difficult to detect, and our size–frequency distribution indicates that specimens  $< 20$  mm are seriously undersampled. Growth in *M. obliqua*, however, is rather slow, and hence the bias in size determination is less serious than it would be in a fast-growing species. Nevertheless, our estimates of productivity ( $0.1 \text{ yr}^{-1}$ ) and production (shelf:  $3.3 \text{ mg } C_{\text{org}} \text{ and } 90.6 \text{ mg ash } m^{-2} \text{ yr}^{-1}$ ; slope:  $0.1 \text{ mg } C_{\text{org}} \text{ and } 3.4 \text{ mg ash } m^{-2} \text{ yr}^{-1}$ ) may underestimate true values. The frequency data refer to shelf stations only (Table 1), and hence their use for slope productivity computations makes the latter figures less reliable.

To our knowledge, these are the first production and productivity figures computed for bryozoans ever, so a comparison between high-Antarctic and other species is not possible. The differences in growth, however, indi-

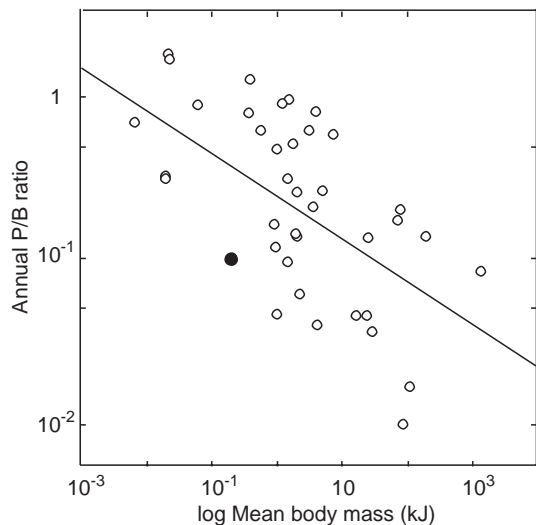


**Fig. 6** Annual  $P/B$  ratio of *Melicerita obliqua* (filled dot) compared with data of other Antarctic species. For data sources see Brey and Clarke (1993), Brey et al. (1995a,b), Kühne (1997)

cate that productivity of *Melicerita obliqua* is lower than that of the species mentioned above. Correcting for differences in mean individual body mass and taking one bryozoan colony as one individual, the  $P/B$  ratio of *M. obliqua* is in the lower range of all Antarctic species investigated so far (Fig. 6).

We did not investigate reproduction or reproductive output, but Winston (1983) found as many as ten embryos per segment in fragments of larger colonies, whereas Androssova (1972) did not find embryos in colonies smaller than 28 mm length. From the size–frequency distribution (Fig. 3) and the size–age relation (Eq. 5), we can infer that the number of segments of appropriate size is about  $100 \text{ m}^{-2}$  on the shelf ( $4 \text{ m}^{-2}$  on the slope), leading to an estimate of maximum reproduction of  $1000 \text{ embryos } m^{-2}$  ( $40 \text{ embryos } m^{-2}$  on the slope) per year.

**Acknowledgements** We would like to thank K. Beyer (*Melicerita* measurements), M. Seebeck (x-ray photography) and G. Traue (ARMS measurements) for technical assistance. This is Alfred Wegener Institute Publication No. 1417.

### References

- Androssova EI (1972) Marine invertebrates from Adelie Land, collected by the XII and YV French Antarctic expedition. 6. Bryozoa. *Téthys* 2 (Suppl): 87–102
- Arntz WE, Brey T, Gerdes D, Gorny M, Gutt J, Hain S, Klages M (1992) Patterns of life history and population dynamics of benthic invertebrates under high Antarctic conditions of the Weddell Sea. In: Colombo G, Ferrari I, Ceccherelli VU, Rossi R (eds) *Marine eutrophication and population dynamics*. Proceedings of the 25th European Marine Biology Symposium. Olsen and Olsen, Fredensborg, Denmark, pp 221–230
- Barnes DKA (1995) Seasonal and annual growth in erect species of Antarctic bryozoans. *J exp mar Biol Ecol* 188: 181–198
- Bathmann U, Fischer G, Müller PJ, Gerdes D (1991) Short-term variations in particulate matter sedimentation off Kapp Nor-

- vegia, Weddell Sea, Antarctica: relation to water mass advection, ice cover, plankton biomass and feeding activity. *Polar Biol* 11: 185–195
- Brey T (1991) Population-dynamics of *Sterechinus antarcticus* (Echinodermata: Echinoidea) on the Weddell Sea shelf and slope, Antarctica. *Antarctic Sci* 3: 251–256
- Brey T, Arntz WE, Pauly D, Rumohr H (1990) *Arctica (Cyprina) islandica* in Kiel Bay (western Baltic): growth, production and ecological significance. *J exp mar Biol Ecol* 136: 217–235
- Brey T, Clarke A (1993) Population dynamics of marine benthic invertebrates in Antarctic and subantarctic environments: are there unique adaptations? *Antarctic Sci* 5: 253–266
- Brey T, Pearse J, Basch L, McClintock J, Slattery M (1995a) Growth and production of *Sterechinus neumayeri* (Echinoidea: Echinodermata) in McMurdo Sound, Antarctica. *Mar Biol* 124: 279–292
- Brey T, Peck L, Gutt J, Hain S, Arntz WE (1995b) Population dynamics of *Magellania fragilis*, a Brachiopoda dominating a mixed-bottom macrobenthic community on the Antarctic shelf. *J mar biol Ass UK* 75: 857–869
- Clarke A, North AW (1991) Is the growth of polar fish limited by temperature? In: Di Prisco G, Maresca B, Tota B (eds) *Biology of Antarctic fish*. Springer, Berlin, pp 54–69
- Cook PL (1985) Bryozoa from Ghana. *Mus r Afr cent Tervuren Belg Ann Ser Octavio Sci Zool* 238: 1–315
- Crisp DJ (1984) Energy flow measurements. In: Holme NA, McIntyre ND (eds) *Methods for the study of marine benthos*. Blackwell Scientific, London, pp 284–372
- El-Sayed SZ (1988) Seasonal and interannual variabilities in Antarctic phytoplankton with reference to krill distribution. In: Sahrhage D (ed) *Antarctic Ocean and resource variability*. Springer, Berlin, pp 101–119
- Emrich K, Erhalt DH, Vogel JC (1970) Carbon isotope fractionation during the precipitation of calcium carbonate. *Earth planet Sci Lett* 8: 363–371
- Epstein S, Buchsbaum R, Lowenstam HA, Urey HC (1953) Revised carbonate-water isotopic temperature scale. *Bull geol Soc Am* 64: 1315–1325
- Gutt J, Starmans A (1998) Megabenthic structure and biodiversity in the Weddell and Lazarev Seas (Antarctic): ecological role of physical parameters and biological interactions. *Polar Biol* (in press)
- Hut G (1987) Stable isotope reference samples for geochemical and hydrological investigations. Report No. 42, International Atomic Energy Agency, Vienna
- Krantz DE, Williams FD, Jones DS (1987) Ecological and paleoenvironmental information using stable isotope profiles from living and fossil molluscs. *Palaeogeogr Palaeoclim Palaeoecol* 58: 249–266
- Kühne S (1997) Solitäre Ascidiens in der Potter Cove (King George Island, Antarktis). Ph.D. thesis, Universität Bremen, Bremen, Germany
- McCrea JM (1950) On the isotopic chemistry of carbonates and a paleotemperature scale. *J chem Phys* 18: 849–857
- Pätzold J, Ristedt H, Wefer G (1987) Rate of growth and longevity of a large colony of *Pentapora foliacea* (Bryozoa) recorded in their oxygen isotope profile. *Mar Biol* 96: 535–538
- Ricker WE (1975) Computation and interpretation of biological statistics of fish populations. *Bull Fish Res Bd Can* 191: 1–382
- Ryland JS (1976) Physiology and ecology of marine bryozoans. *Adv mar Biol* 14: 285–443
- Salonen K, Sarvala J, Hakala I, Viljanen M-L (1976) The relation of energy and organic content in aquatic invertebrates. *Limnol Oceanogr* 21: 724–730
- Schalk PH, Brey T, Bathmann U, Arntz W, Gerdes D, Diekmann G, Ekau W, Gradinger R, Plötz J, Nöthig E, Schnack-Schiel SB, Siegel V, Smetacek V, Van Franeker JA (1993) Towards a conceptual model for the Weddell Sea ecosystem. In: Christensen V, Pauly D (eds) *Trophic models of aquatic ecosystems*. ICLARM Conference Proc. 26, ICLARM, Manila, pp 323–337
- Smetacek V, Scharek R, Nöthig E (1990) Seasonal and regional variation in the pelagic and its relationship to the life history of krill. In: Kerry KR, Hempel G (eds) *Antarctic ecosystems*. Springer, Berlin, pp 103–114
- Stebbing ARD (1971) Growth of *Flustra foliacea* (Bryozoa). *Mar Biol* 9: 267–273
- von Bodungen B, Smetacek V, Tilzer MM, Zeitschel B (1986) Primary production and sedimentation during spring in the Antarctic peninsula region. *Deep-Sea Res* 33: 177–194
- Wefer G, Berger WH (1991) Isotope paleontology: growth and composition of extant calcareous species. *Mar Geol* 100: 207–248
- Winston JE (1983) Patterns of growth, reproduction and mortality in bryozoans from the Ross Sea, Antarctica. *Bull mar Sci* 33: 688–702